Comparison of thermoelectric properties of GaN and ZnO samples

B. Kucukgok[*1], B. Wang[2], A. G. Melton[1], N. Lu[3], and I. T. Ferguson[1]

[1] Department of Electrical and Computer Engineering, University of North Carolina at Charlotte, 9201 University City Blvd., Charlotte, NC 28223, USA

[2] College of Information Science and Engineering, Hebei University of Science and Technology, 70 Yuhua East Rd., Shijiazhuang, Hebei 050018, P.R. China

[3] Department of Engineering Technology, University of North Carolina at Charlotte, 9201 University City Blvd., Charlotte, NC, USA

In this paper, room temperature thermoelectric (TE) properties of wide bandgap thin film GaN and bulk ZnO are studied. Bulk GaN is also incorporated with epitaxy films to make comparison. GaN and ZnO materials have superior electrical performance and chemical stability at high temperatures and are currently found in many commercial applications, such as, photovoltaic, solid-state lighting, and gas sensors. Since there are not many semiconductor materials that can operate effectively at high temperatures, wide bandgap materials like GaN and ZnO would be a promising solution for high temperatures thermoelectric power generation. In order to understand their TE properties, we systematically compared and characterized TE behaviour of GaN and ZnO thin films with a function of doping concentrations. The common trend of a decrease in Seebeck coefficients with the increase of carrier concentration for thin film and bulk GaN is observed, however, reverse TE trend for bulk ZnO, were observed. The most commonly observed TE trend is attributed to Mott-Jones relation to simple transport models while inverse trend could be suggested as hopping conductance. Moreover, the Seebeck coefficients of ZnO samples are found to be larger than those of thin film and bulk GaN samples in the similar carrier density. Highest power factors, 2.6×10^{-4} W/mK^2 and 0.65×10^{-4} W/mK^2, and Seebeck coefficients, 478 µV/K and 481 µV/K were measured for thin film GaN and bulk ZnO, respectively.

1 Introduction Thermoelectric (TE) energy can directly produce electrical power from waste heat harvesting due to Seebeck effect. This phenomenon, a temperature gradient across a solid produce an electromotive force between the hot and cold end, discovered in 1821 by Thomas Johann Seebeck [1-7]. Therefore, a wide variety of TE application for waste heat harvesting can be found in automobiles (heat seat and gas exhaust), woodstove, spacecraft by generation of energy using of radioisotope thermoelectric generators (RTGs), solar cells, and computer chips [1-9]. Although the efficiency of TE devices is lower than that of conventional energy sources as electric generators and/or refrigerators, for last two decades researches have shown that using new state-of-the-art TE materials high efficiency TE devices could be achieved [1-18] and replaced by current technology. The widely used TE materials for power generation are Bi$_2$Te$_3$, PbTe, and Si$_{1-x}$Ge$_x$ for room and high temperature applications [4, 7-11], however the commercial application of these materials are limited due to their volatility, toxicity (Te based element), and poor stability at high temperatures [12-14]. Therefore, recent research effort have mostly been focusing on developing new TE materials, which are non-toxic, easily reproducible, and more importantly have superior thermal stability at high temperature ranges.

Wide bandgap materials are promising candidate for high temperature TE materials because they are thermally and chemically stable at these temperatures, while maintaining good electrical performance. Recently, wide bad gap materials; GaN and its alloys and ZnO especially Al doped ZnO have demonstrated promising results as high efficiency TE materials [13-18, 20, 22-24]. GaN-and ZnO-based wide bandgap materials have shown superior electrical and mechanical performance at high temperatures, high density-

Phys. Status Solidi C **11**, No. 3–4 (2014)
895

Contributed

Article

of-states (DOS)-mobility products, which lead to high power factors. Therefore, these materials are widely used in commercial applications including solid-state lighting, solar cells, transistors, laser diodes, and gas sensors [14-17, 20-24].

In previous studies numerous groups have studied TE properties of III-Nitrides and its alloys and ZnO materials (ceramic and powder) [1-18, 20-24]. However, in the present study, as a first group, we investigated the detail work of comprising the TE properties bulk ZnO with HVPE grown bulk GaN and MOCVD grown thin film GaN. The current study also extends and improves upon our previous work [13] by including TE properties of bulk ZnO.

2 Interrelationships between TE coefficients and TE materials

2.1 Conversion efficiency and figure of merit, *ZT*

The conversion efficiency of a TE devices is found by the Carnot efficiency and the figure of merit, *ZT* as shown;

$$\eta = \left(\frac{T_{hot} - T_{cold}}{T_{hot}} \right) \left(\frac{\sqrt{1 + ZT_m} - 1}{\sqrt{1 + ZT_m} + \left(\frac{T_{cold}}{T_{hot}} \right)} \right) \quad (1)$$

where the Carnot efficiency is the temperature differences of hot and cold sides over temperature at hot side, and T_m is the mean temperature [3,4]. The TE figure of merit,

$$ZT = \frac{s^2 T}{p\kappa} = \frac{PF}{\kappa} = \frac{s^2 T}{p(\kappa_l + \kappa_e)} \quad (2)$$

where S is the Seebeck coefficient, σ is the electrical conductivity, κ is the thermal conductivity, and T is the absolute temperature [6, 13-16]. A good TE material requires a high Seebeck coefficient, high electrical conductivity, and a low thermal conductivity. Improving ZT for mature TE materials is challenging due to the interdependence of the properties contributing to Z, i.e. S, σ, and k. For instance, For example, the thermal conductivity κ, is the sum of two contributions, the electronic thermal conductivity κ_e (due to electron and hole transport) and the lattice thermal conductivity κ_L (due to phonon transport). The Wiedemann-Franz Law ($\kappa_e = L\sigma T$, where L is Lorenz constant) shows that the electrical conductivity (σ) increases linearly with the electronic thermal conductivity (κ_e), whereas the lattice thermal conductivity (κ_L) is independent of the electronic properties. Thus, improving TE performance in a semiconductor mostly focus on either degrading lattice thermal conductivity or increasing Seebeck coefficient as seen in Eq. (3) and (4). It can be seen from Mott-Jones relation to simple transport models [12,18],

$$S = \frac{k}{e} \left(r + \frac{5}{2} + \ln \frac{Nc}{n} \right) \quad (3)$$

$$N_c = 2 \left(\frac{2\pi m^* kT}{h^2} \right)^{3/2} \quad (4)$$

where N_c, n, r, k, m^*, and h are the effective density of states (DOS) at the Fermi level, carrier concentration, and a factor related to scattering mechanism, boltzman constant, DOS effective mass, and planck constant respectively. Thus, above equations pointed out that figure of merit, *ZT* is not only determined by doping alone but also have incorporation with m^* without degenerating mobility (μ) [4].

2.2 New TE materials

Several researches have been focused and studied in detail with using bulk materials, such as, skutterudites, clathrate, half-Heusler alloys, and complex chalcogenides [7-12]. Recently, new TE materials as oxides, nitrides in both nanocomposites, and thin film have been proposed and became play a crucial role to enhance high *ZT* value of TE materials [7-18]. A new concept was first proposed by Slack *et al.* for TE material to achieve high *ZT* value (low conductivity (σ) and low thermal conductivity (κ)) "phonon glass electron crystal" (PGEC) [19]. At low temperatures narrow bandgap materials may be used, which have inherently high electrical conductivity and low thermal conductivity. However, because of their narrow bad gap, they have limited thermal stability. The semiconductors with badgap (E_g) > $10k_BT$ make good TEs for high temperature operations, where k_B is the Boltzmann constant and T is the absolute temperature, to prevent the excitation of minority carriers and the loss of the n- or p-type character of the material [4,8]. As a result, oxides and nitrides have recently begun to attract more attention as promising high temperature TE materials. Since Ohtaki *et al.* first demonstrated sintered $Al_{0.02}Zn_{0.98}O$ and showed quite promising TE behaviours of oxide TE materials [6], many studies has started to focus on TE of oxide based structures and devices including n- and p-type oxides, and ZnO [1-7].

3 Experimental The samples studied here were thin film GaN, bulk GaN and ZnO samples. Thin GaN samples with various doping concentrations were grown on c-axis 2 in. sapphire wafer by metal organic vapour deposition method (MOCVD). The "bulk" GaN samples were around 400-μm- thick materials grown by high-vapor-pressure (HVPE) epitaxy on sapphire, with the substrate lapped off by Kayma Inc. Zn face of (0001) bulk ZnO samples were provided from Cermet Inc. The thicknesses of thin film GaN and bulk ZnO samples were around 2 μm and 400 μm, respectively. The standard Seebeck measurement, thermal gradient method was used to determine Seebeck coefficients by placing the sample across two commercial thermoelectric modules which one module was heating one end of the sample while other one, on the other end of the sample, was held at constant temperature during measurements. The detail procedure and sample preparations can be found in detail in elsewhere [13]. The electrical charac-

terizations were performed by Van der Pauw Hall-effect measurement methods in the in-plane direction. Moreover, errors in Vander Pauw Hall and Seebeck measurements are estimated at ± 10% and are induced by error in thermocouple temperature measurements and probe Seebeck voltage. Additionally ±5% error is estimated for film thickness measurements [15].

4 Results and discussion

4.1 Seebeck and electrical properties of thin film GaN, bulk GaN
Figures 1(a) and 1(b) show Seebeck coefficient (S) and power factor ($S^2\sigma$) of thin film and bulk GaN and ZnO as a function of carrier concentration (n) at room temperature, respectively. As n increases both thin film and bulk GaN show decreasing trend with respect to S, which is the normal TE behaviour according to Eq. (3) and (4). All the thin film GaN samples showed negative Seebeck coefficient indicating n-type conduction as a consequence of Si doping of GaN (The absolute value of S is shown in all graphs for clear representation.) The GaN thin film and bulk samples also exhibit linear dependence of S while n increases. As shown, high S value does not compensate low electrical conductivity at lower doping concentration. The dependence of power factor on carrier density is illustrated in Fig. 1(b). As n increases power factor of thin film first increases and then decreases except one point which is at 1.6×10^{18} cm^{-3}. The reason of peak power factor point at 1.6×10^{18} cm^{-3} can be attributed to major trade-off between Seebeck coefficient and electrical conductivity and Seebeck coefficient's dominant role on determining power factor, which is depicted as "$S^2\sigma$". The observed trends in Fig. 1(a) and (b) for thin film and bulk GaN are in agreement with previous experimental and theoretical studies of nitride based semiconductors [15, 16, 22]. At high carrier density (above 10^{18} cm^{-3}) Seebeck coefficient of the n-type GaN samples lowers significantly (Fig. 1(a)), which results in low power factor (Fig. 1(b)). Moreover, the highest power factor was found 2.6×10^{-4} W/mK^2 at 1.6×10^{18} cm^{-3} and ~0.35 $\times 10^{-4}$ W/mK^2 at 2.4×10^{18} cm^{-3} for thin film GaN and bulk GaN, respectively. Additionally, the highest absolute Seebeck coefficient, 478 µV/K, was measured at around 4.2×10^{16} cm^{-3} for thin film GaN whereas 313 µV/K was found at same order of magnitude carrier density for bulk GaN. We attentively attribute this to different dislocation densities of MOCVD grown thin films and HVPE grown bulk GaN. In this study, the dislocation densities of the bulk and thin film GaN samples are around 10^8 and 10^{10} cm^{-3}, respectively. Since MOCVD thin film GaN samples were grown on sapphire substrate, the high dislocation density induced by large lattice mismatch and strain between GaN and sapphire result in enhanced scattering related factor (r) and lead to high S values according to Eq. (3). The details about dislocation calculation and its effect on S of thin film and bulk GaN can be found in our previous study [13]. This mechanism also has an influence over electrical
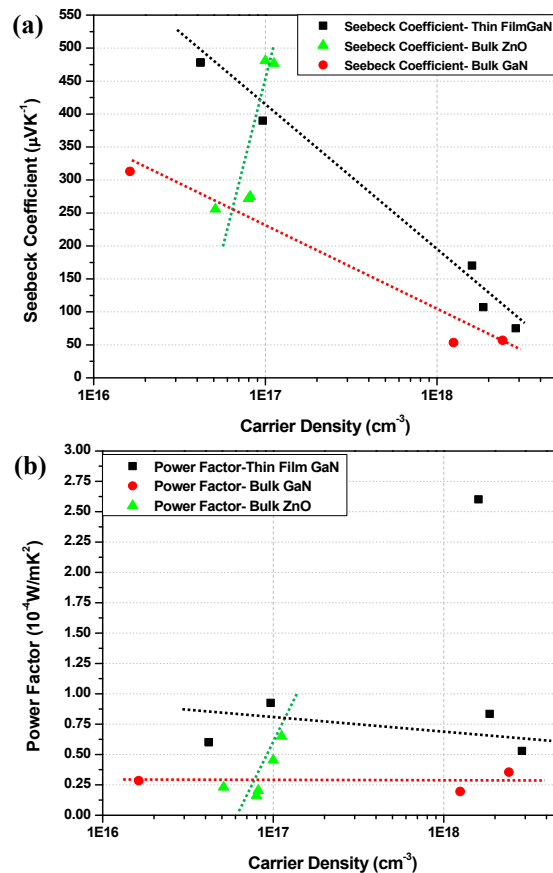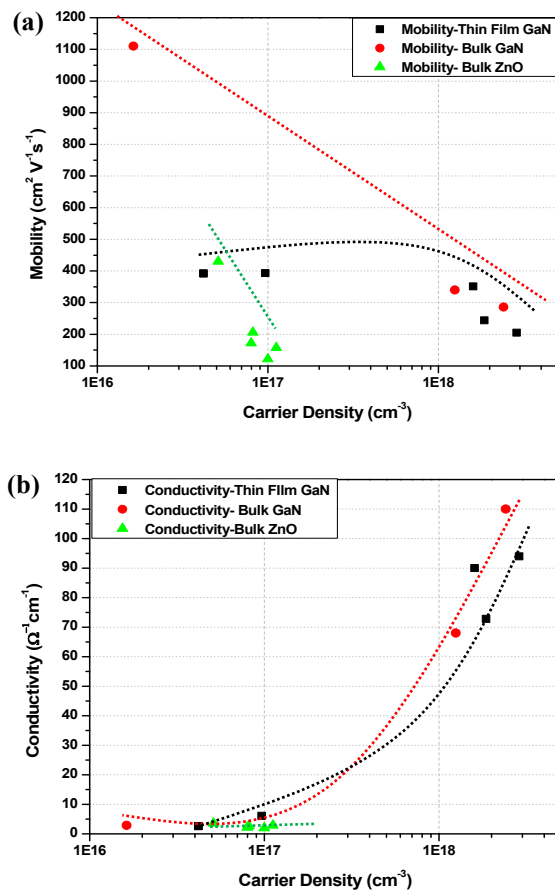

Figure 1 (a) Seebeck coefficient vs. carrier concentration at room temperature (300 K): thin film GaN, bulk ZnO, and bulk GaN. (b) Power factor as a function of carrier concentration at room temperature (300 K): thin film GaN, bulk ZnO, and bulk GaN. Dashed lines are guided to the eye.

properties of thin GaN as seen in Figs. 2(a) and (b). Figures 2(a) and 2(b) depict behaviour of mobility µ and conductivity σ as a function of n. For thin film and bulk GaN µ decreases and σ increases as n increases. In Fig. 2(a) for thin film GaN samples, limitation of mobility drop at around low carrier densities, 10^{16}-10^{17} cm^{-3} could be attributed to ionized impurity scattering, which does not play a major role on bulk GaN. Additionally, in Fig. 2(a) in the range of 10^{16} cm^{-3}, the mobility gap between thin film GaN and bulk GaN was high. This could be attributed to the impact of scattering, which simultaneously lowers µ while enhances S.

4.2 Seebeck and electrical properties of bulk ZnO
S and $S^2\sigma$ bulk ZnO with respect to n is shown in Fig. 1(a) and 1(b). Unlike the trend observed in GaN, bulk ZnO shows inverse TE behaviour of that S increases as n increases. The abnormal S behaviour can be attributed to hopping conductance [1, 12, 17] because hopping conductance surpasses the σ and S does not decrease [12] and it may be noted here that higher effective masses usually brings out higher DOS, lower µ, and higher S [16]. Moreover, enhance relaxation time of carriers due to the better

(a)

(b)

Figure 2 Mobility vs. carrier concentration at room temperature (300 K): thin film GaN, bulk ZnO, and bulk GaN. (b) Conductivity a function of carrier concentration at room temperature (300 K): thin film GaN, bulk ZnO, and bulk GaN. Dashed lines are guided to the eye as.

crystal quality can be attributed to have larger Seebeck coefficient with increasing carrier concentration [17]. Mobility so that conductivity of bulk ZnO is lower than thin film and bulk GaN at carrier density at 10^{17} cm^{-3} (excluding one sample) as seen from Figs. 2(a) and (b). This could be attributed to possess slightly difference of bond lengths, 1.95 and 1.97 Å for Ga-N and Zn-O atoms, respectively, and also effective masses $0.2m_e$ and $0.23m_e$ for GaN and ZnO, respectively [20, 21]. Larger bond length leads to lattice strain and enhances native defects. Since mobility strongly relies on the density of defects and effective mass this may result in low electron mobility and thus conductivity [14, 21].

5 Conclusion In summary, TE properties of thin film and bulk GaN and bulk ZnO were examined. The highest Seebeck coefficients were found 481 µV/K and 478 µV/K for bulk ZnO and thin film GaN at carrier density of 10^{16} cm^{-3}, respectively. Additionally, highest power factors were measured as 0.65×10^{-4} W/mK^2 and 2.6×10^{-4} W/mK^2, for bulk ZnO and thin film GaN, respectively. The value of power factor of both materials exceeded that of SiGe at

same temperature. III-nitrides and oxides materials will play important role as a promising TE materials and devices in near future.

References

[1] M. Ohtaki, J. Ceram. Soc. Jpn. **119**, 770-775 (2011).
[2] J. W. Fergus, J. Europ. Soc. **32**, 525-540 (2012).
[3] K. Koumoto, R. Funahashi, E. Guilmeau, Y. Miyazaki, A. Weidenkaff, Y. Wang, and C. Wan, J. Am. Ceram. Soc. **96**, 1-23 (2013).
[4] J. He, Y. Liu, and R. Funahashi, J. Mater. Res. **26**, 1762 (2011).
[5] G. Homm, F. Gather, A. Kronenberger, S. Petznick, T. Henning, M. Eickhoff, B. K. Meyer, C. Heiliger, and P. J. Klar, Phys. Status Solidi A **210**, 119 (2013).
[6] M. Ohtaki, T. Tsubota, K. Eguchi, and H. Arai, J. Appl. Phys. **79**, 1816 (1996).
[7] L. Li, L. Fang, X. J. Zhou, Z. Y. Liu, L. Zhao, and S. Jiang, J. Electron Spectrosc. Relat. Phenom. **173**, 7 (2009).
[8] A. J. Minnich, M. S. Dresselhaus, Z. F. Ren, and G. Chen, Energy Environ. Sci. **2**, 466-479 (2009).
[9] H. Alam and S. Ramakrishna, Nano Energy **2**, 190 (2013).
[10] Y. Takagiwa, Y. Pei, G. Pomrehn, and G. J. Snyder, Appl. Phys. Lett. **101**, 161904 (2012).
[11] Q. Zhang, H. Wang, Qian. Zhang, W. Liu, B. Yu, H. Wang, D. Wang, G. Ni, G. Chen, and Z. Ren, Nano Lett. **12**, 2324 (2012).
[12] S. Yamaguchi, Y. Iwamura, and A. Yamamoto, Appl. Phys. Lett. **82**, 2065 (2003).
[13] B. Wang, B. Kucukgok, Q. He, A. Melton, J. Leach, K. Udwary, K. Evans, N. Lu, and I. T. Ferguson, Proc. 2013 MRS Spring Meeting & Exhibit., April (2013).
[14] M. Kamano, M. Haraguchi, T. Niwaki, M. Fukui, M. Kuwahara, T. Okamoto, and T. Mukai, Jpn. J. Appl Phys. **41**, 5034 (2002).
[15] A. Sztein, J. E. Bowers, S. P. DenBaars, and S. Nakamura, J. Appl. Phys. **112**, 083716 (2012).
[16] A. Sztein, H. Ohta, J. E. Bowers, S. P. DenBaars, and S. Nakamura, J. Appl. Phys. **110**, 123709 (2011).
[17] J. Zhang, S. Kutlu, G. Liu, and N. Tansu, J. Appl. Phys. **110**, 043710 (2011).
[18] M. S. Brandt. P. Herbst, H. Angerer, O. Ambacher, and M. Stutzman, Phys. Rev. B **58**, 7786 (1998).
[19] G. A. Slack, CRC Handbook of Thermoelectrics, edited by D. M. Rowe (CRC Press, Boca Raton, 1995), p. 407.
[20] T. Hanada, Oxide and Nitride Semiconductors (Springer, Berlin, Heidelberg, 2009), p. 1.
[21] Ü. Özgür, Ya. I. Alivov, C. Liu, A. Teke, M. A. Reshchikov, S. Doğan, V. Avrutin, S.-J. Cho, and H. Morkoç, J. Appl. Phys. **98**, 041301 (2005).
[22] W. Wen-Tao, W. Ke-Chen, M. Zu-Ju, S. Rong-Jian, W. Yong-Quin, and L. Qiao-Hong, Chin. J. Struct. Chem. **31** (2012).
[23] H. Tong, J. Zhang, G. Liu, J. A. Herbsommer, G. S. Huang, Appl. Phys. Lett. **97**, 112105 (2010).
[24] B. N. Pantha, I.-W. Feng, K. Aryal, J. Li, J.-Y. Lin, and H.-X. Jiang, Appl. Phys. Express **4** (2011).